



**HAL**  
open science

## Detecting potential temperature defects on harness of cables with reflectometry

Nicolas Gregis, Mickaël Cartron, Mariem Ben Hadj Abdallah, David Monchaux, Dominique Besson

► **To cite this version:**

Nicolas Gregis, Mickaël Cartron, Mariem Ben Hadj Abdallah, David Monchaux, Dominique Besson. Detecting potential temperature defects on harness of cables with reflectometry. EUCASS-3AF 2022 - 9 European conference for aeronautics and space sciences, Jun 2022, Lille, France. pp.10.13009, 10.13009/EUCASS2022-6144 . cea-04239486

**HAL Id: cea-04239486**

**<https://cea.hal.science/cea-04239486>**

Submitted on 12 Oct 2023

**HAL** is a multi-disciplinary open access archive for the deposit and dissemination of scientific research documents, whether they are published or not. The documents may come from teaching and research institutions in France or abroad, or from public or private research centers.

L'archive ouverte pluridisciplinaire **HAL**, est destinée au dépôt et à la diffusion de documents scientifiques de niveau recherche, publiés ou non, émanant des établissements d'enseignement et de recherche français ou étrangers, des laboratoires publics ou privés.

# Detecting potential temperature defects on harness of cables with reflectometry

*Nicolas Grégis\*, Mariem Slimani\*, Mickaël Cartron\**

*\* Université Paris-Saclay, CEA, List, F-91120, Palaiseau, France*

*David Monchaux<sup>2</sup>, Dominique Besson<sup>2</sup>*

*<sup>2</sup> Centre National d'Etudes Spatiales (CNES), 52 rue Jacques Hillairet, 75612 Paris Cedex, France*

## Abstract

In this paper, we propose a new model taking into account local thermal effect on the cable. A thinner modelling combining the ABCD frequency method with a mesh description of the network is used to analyse the effect of a progressive temperature profile on the cable. Two cases were considered : a drastic drop and an important raise of the temperature. Numerical simulations and reflectometry experimental measurements were conducted to validate the new model. Great similarities were observed and reflectometry sensors showed that hot and cold spots can be detected and located.

## 1. Introduction

In a context of Reusable Launch Vehicles (RLV), preventive maintenance is the solution to ensure reliable and safe reuse of the system for extending its useful life. In particular, cables are critical components of the space launch system subject to harsh environmental conditions such as mechanical stress, heat, vibration etc., which can lead to severe damage and affect the overall functionality of the system. In [1], we proposed a monitoring system, based on electrical reflectometry technique, where embedded sensors are deployed on the harness of the vehicle. We showed, through numerical simulations based on a rough model that thermal defects can be detected. However, this model integrates only brutal temperature change and does not considers progressive temperature variations along the cable.

In this study, we propose more accurate models, taking into account local thermal effect on the cable. We included in the ABCD frequency method a mesh description of the cable to allow a thinner modelling while considering a progressive temperature profile. We proposed a combination of a mesh description and the ABCD calculus method where the mesh's parameters are optimized to reduce side effects on simulations. Using a previously given law linking temperature variations and materials variations, we could generate the impact on reflectometry for each cell of the mesh and mitigate the unwanted reflections created by this new model.

Then, two cases were considered. First, we focused on a dramatic drop of the temperature on a local part of the cable, for temperatures ranging from -50 °C to -200 °C. This can happen, for example, when the thermal protection around the propellant tanks is damaged and the cable is exposed to very low temperature. Second, we considered an important raise of the temperature of a part of a cable up to 180°C, as it could happen with the presence of a hot spot near a rocket engine, for instance.

For both cases, numerical simulations were conducted taking into account a cable network used for power distribution with the presence of local thermal defects in different places of the cable. The topology of the network and the wanted experimental set-up are modelled in the simulation tools to be as close as possible to the conditions used for real testing. To prove the validity of the proposed models, experimental test beds were set to reproduce the same scenario as in simulation. For low temperatures, we immersed part of a cable in a tank full of liquid nitrogen. We equipped the cable with temperature sensors and used a reflectometry measurement tool. We then measured TDR signals. In addition, an oven was used to locally heat a portion of the cable. Reflectometry measurements based on the new simulation models are compared to experimental results and great similarities between the simulations and the measurements are observed. The response of reflectometry sensors shows that hot and cold spots can be detected and located.

All this work provides an experimental validation of a newly designed model describing the cable damage due to local temperature change, and lays the proof of the capability of our reflectometry sensors to detect and locate such types of defects on a typical cable used in Space Launch Vehicles.

This paper is organised as follows. In section 2, a brief review of reflectometry-based method is presented. Section 3 recalls the basis of ABCD modelling. In Section 4, we describe a mixed approach based on the combination of a mesh description and the ABCD modelling allowing the mitigation of simulation side-effects. Experimental set-up is described in Section 5. In Section 6, we report experimental TDR measurements for the two considered cases. Section

7 compares simulations based on the new mesh description modelling to experimental results. Finally, concluding remarks are drawn in Section 8.

## 2. Principle of reflectometry

Reflectometry is a well-known technique in electromagnetics that has been widely used for locating and detecting faults in cables. Reflectometry methods are based on the injection of a test signal down the medium and the analysis of the reflected signal, generated due to the impedance mismatch or discontinuities encountered in its propagation path. Reflectometry methods can be classified into two main families: Time Domain Reflectometry (TDR) [1] and frequency Domain Reflectometry (FDR) [2]. The main difference between these two families lies on the injected stimulus waveform and the reflected signal processing techniques. TDR techniques send a pulse into the medium which travels through it with a propagation velocity related to cable physical characteristics. The incident waveform reflects back when it encounters any impedance discontinuity. The propagation of a wave along a cable is modelled using the 4-parameter RLCG model (resistance, inductance, capacitance, and conductance per unit length) which is frequency dependent. The reflection coefficient ( $\varphi$ ) that represents the ratio between the reflected signal and the incident signal can be seen as an index of discontinuity impedance and can be obtained as follows:

$$\varphi = \frac{Z_d - Z_c}{Z_d + Z_c} \quad (1)$$

Where  $Z_d$  represents the impedance of the discontinuity and  $Z_c$  is the characteristic impedance of the line that can be given as a function of the angular frequency  $\omega$  as follows:

$$Z_c(\omega) = \sqrt{\frac{R + jL\omega}{G + jC\omega}} \quad (2)$$

The propagation constant  $\gamma$ , representing the attenuation and the phase change of the wave as it propagates is also dependent on the RLCG characteristics of the cable and is defined as follows :

$$\gamma(\omega) = \sqrt{(R + jL\omega)(G + jC\omega)} \quad (3)$$

TDR has the advantage to generate a simple reflectogram easier to understand and analyse as the peaks are naturally linked to the faults or discontinuities present on the cable. Figure 1 shows a TDR reflectogram where the first peak corresponds to the mismatch between the reflectometer and the cable under test and the second peak represents the open circuit at the end of the cable. The open circuit fault can be located as follows:

$$d = \tau * v_p$$

Where,  $v_p$  is the propagation speed through the cable and  $\tau$  is the round trip travelling time between the injection point and the fault.

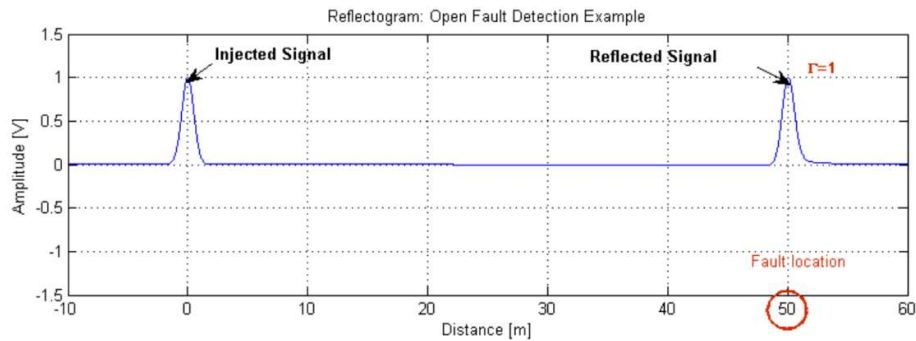


Figure 1: Reflectogram with and open circuit at the end of the cable [3].

### 3. ABCD modelling

ABCD method is a frequency description method, commonly used to model electrical system considered as a connection of cascaded two-port networks. Each two-port network can be characterized by its ABCD parameters, also known as chain parameters or scattering parameters, describing the relationship of the input voltage and current to the output voltage and current of the two-port network. The overall scattering parameters of the whole system can be obtained from the ABCD parameters of each two-port network in the cascade which are multiplied with each other. The transfer function of the complete system can be then deduced from the calculated ABCD chain knowing the boundary conditions (terminal constraints).

This method has a large number of advantages. First, it is the easiest way to calculate the transfer function of the system as it simplifies complex calculations to matrix products. Moreover, it allows to get the response of the system as a function of the frequency of the input stimulus.

In reflectometry, a cable can be modelled as a transmission line characterized by its ABCD matrix if the propagation conditions are homogeneous over the entire length of the line. A cable network can be modelled as a cascade of uniform sections characterized by its scattering parameters where its section respects the condition mentioned above. The ABCD parameter matrix of a general uniform transmission line is given as follows:

$$M = \begin{pmatrix} A & B \\ C & D \end{pmatrix} \quad (4)$$

Where,

$$A = \cosh(\gamma l) \quad (5)$$

$$B = \frac{\sinh(\gamma l)}{Z_c} \quad (6)$$

$$C = Z_c \sinh(\gamma l) \quad (7)$$

$$D = \cosh(\gamma l) \quad (8)$$

The losses introduced by the conductors and the dielectric material of the cable are taken into account the propagation factor  $\gamma$ , which is frequency dependent. This propagation constant as well as the characteristic impedance  $Z_c$  are related to the (R, L, C, G) parameters of the cable which are functions of the cross-sectional geometry of the transmission line and the electromagnetic properties of the materials constituting the cable.

As previously said, the use of ABCD parameters supposes a cascade of uniform sections that can model a lossy non-uniform transmission line. This can be used to model a chaining of cables of different types or a sudden change in impedance, for instance. But it is not very suitable to model continuous changes along a cable as it is the case in this study. As a matter of fact, in this work, we investigate the impact of a temperature profile on the physical properties of the cable, which is a continuous process.

In [1] we did a previous work on the detection of hot spot on harness of cables with reflectometry methods using ABCD simulations. We pointed out the feasibility of detecting a hot spot of different lengths and severities in a context of on-line monitoring, but we were limited to the classical ABCD method described here. For short defect (smaller than 15 cm), the detection was particularly close to noise level and was highly dependant of the chosen hypotheses. The previous limitations of the ABCD method and the simulation-only based scenarios raised the question of the confidence level put in the results and the level of detection reachable in reality.

#### 4. Mixed approach with an improved modelling

To tackle this problem and validate our previous results, we proposed in this work to combine the power of an experimental test and the improvement of the ABCD modelling to better describe the temperature profile on the cable and conclude on the detection of defects.

For the simulation modelling, we propose considering the continuous profile of the temperature as a series of step of constant temperature. With this approximation, the cable can be represented as a cascade of small uniform sections with different ABCD parameters each. Each ABCD part are linked to an (R,L,C,G) description model, which is dependent on temperature changes as presented in equation (9). This way, instead of having a sudden change at one point of the cable, we get a more progressive variation of the propagation parameters along the cable, and thus along the temperature profile.

$$\begin{cases} R = 2\sqrt{\frac{\mu\rho f}{\pi}}/\sqrt{1-\frac{d^2}{D^2}} \\ L = \frac{\mu}{2\pi}a\ln\left(\frac{2D}{d}\right) \\ C = 2\pi\varepsilon/\ln\left(\frac{2D}{d}\right) \\ G = 2\pi f\tan(\delta)C \end{cases} \quad (9)$$

Where  $\mu$  is the permeability of the conductor,  $f$  is the frequency,  $d$  is the inner diameter of the conductor,  $D$  is the distance between the two conductors of each braid,  $a$  is a form factor,  $\varepsilon$  is the permittivity of the dielectric component and  $\delta$  is the loss angle of this dielectric.

The principle of the ABCD mesh modelling as a function of the temperature profile is presented on Figure 2.

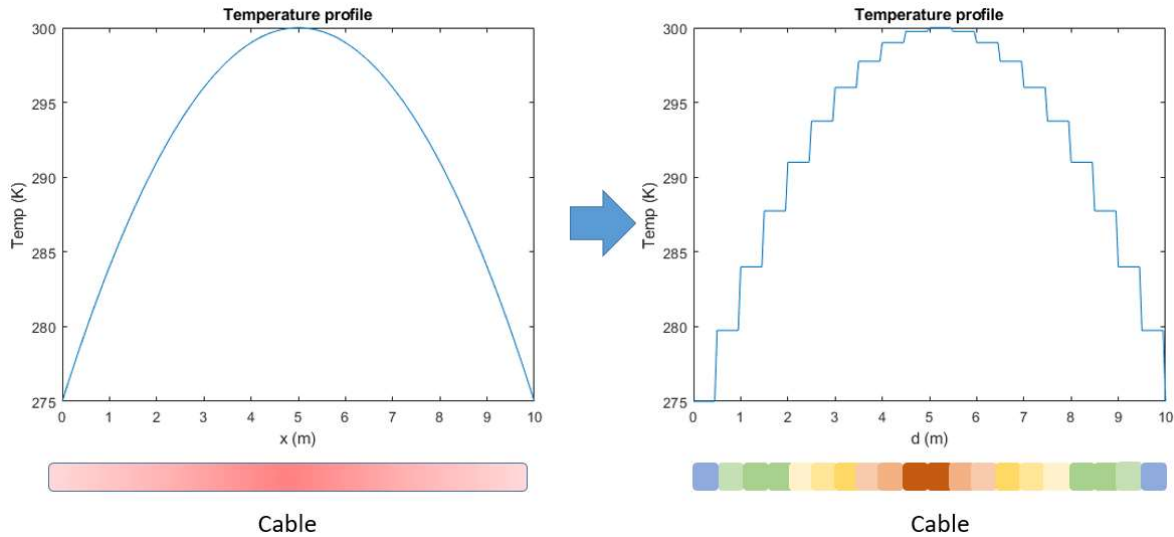


Figure 2: Presentation of the principle of the ABCD mesh.

This approach allows to get the desired profile, but raises several important questions. First, the convenient mesh-fineness should be defined to get accurate results without drastically increasing the computation time. Moreover, the division into multiple uniform sections induces a discontinuity between each element generating some reflections that makes the analysis of the reflectograms more difficult. Those reflections are purely mathematical constructs and depend on the mesh-fineness (amplitude, numbers ...).

We conducted some simulations in order to get an answer to the questions raised above. We simulated a 10 meter-long cable with a variation of temperature as described in Figure 2. We repeated the simulation for different sizes of the mesh, using a step method to approximate the chosen temperature profile. The thinner the mesh, the smaller the step of temperature and thus the variation of RLCG parameters between two parts of the cable.

Figure 3 presents the TDR results for different mesh fineness. Like expected, we can see important oscillations on the curves that disappear progressively when the mesh becomes thinner. In this example, there is almost no noise left when we reach 1/50 of the total length of the cable.

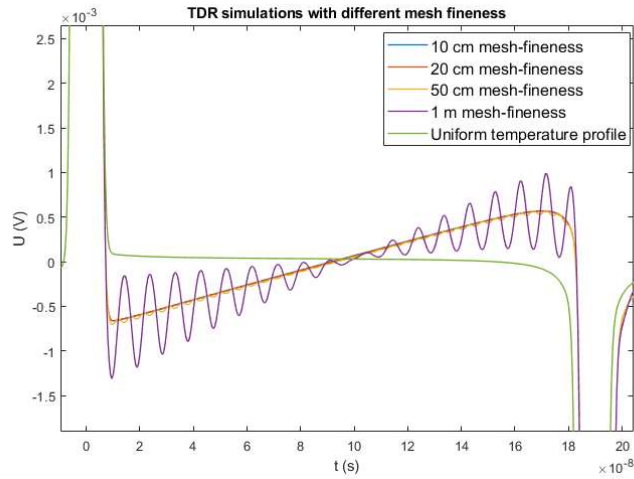


Figure 3: TDR response based on ABCD mesh modelling.

We calculated the computation time for this example, shown in Figure 4. The simulation was conducted using a I7 Intel core with Matlab software. We observe how the time increases with the number of elements in the mesh. So clearly, we have lost in the computation time comparing to ABCD modelling method but this enabled us to efficiently describe a cable under temperature stress and have better results than ABCD description technique.

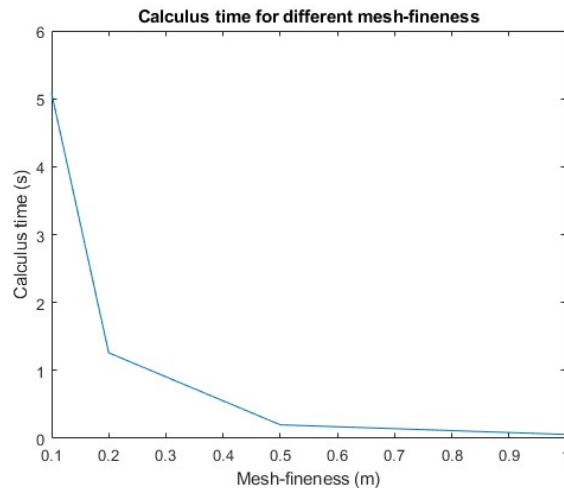


Figure 4: Computation time as a function of mesh-fineness.

As rule of thumb, taking a mesh-fineness of 1/50 of the length of the cable represents a good trade-off that reduced the mathematical noise under 1/100 of the useful signal and kept the simulation time under the time of other simulation

methods, such as FDTD or 3D modelling. The proposed model has been validated based on experimental set-up that will be described in the next section.

## 5. Experimental set-up

In our previous work, we took two hypotheses of temperature for the stressed part of the cable. We modelled a cold spot with temperatures lower to  $0^{\circ}\text{C}$  and then we modelled a hot spot with temperature above  $0^{\circ}\text{C}$ . The extreme cases tested a low temperature of  $-73^{\circ}\text{C}$  and a high temperature of  $+100^{\circ}\text{C}$ .

We designed an experimental set-up that recreates similar tested conditions; using two tools for reflectometry measurements (see Figure 5). The first one is a Vector Network Analyser (VNA) E5072A from the manufacturer Keysight, which is equipped with a Time Domain module for TDR measurements. The second one is a CEA-made TDR sensor consisting of an FPGA based electronic board with a Digital to Analog Converters (DAC) and an Analog to Digital Convertors (ADC). This board allows the generation of a current pulse, the acquisition of the reflected signal and the processing of the signal to detect/ locate defaults in the cables. It is close to the proposed architecture in [1]. Here, the VNA serves as a reference measurement tools, thanks to its high precision response. The CEA-Sensor is used in order to get measurement closer to operational conditions and anticipate the capabilities of embedded sensors for online monitoring.



Figure 5: TDR measurement tools: (a) a Vector Network Analyser (VNA) , (b) CEA TDR sensor.

The characteristics of each TDR measurement tool are summarized in Table 1.

Table 1: Characteristics of TDR measurement tools.

Tool	Time resolution	Number of points	Number of means	Temporal window
VNA	0.5 ns	20001	10	10 $\mu\text{s}$
Ariane V2	1.25 ns	1024	64	1.28 $\mu\text{s}$

We could not have the exact same operation conditions as in [1] so we tried to be as close as possible. We chose for the cable under test a 5m-long shielded twisted pair of copper conductors (SP 359/1871-871) from Filotex manufacturer with an N-type connector on both ends, mounted between the two conductors. This kind of cable is often used in aircrafts and in power transmission. It is chosen for this experiment because it is the closest reference to cables used for launch vehicles and is also close to the one used in [1]. The cable is connected to the measurements tools through a 0.5 m long coaxial cable of type RG58.

To measure the temperature along the cable, we installed temperature probes made with thermocouples RS Pro, type K. Each probe is connected to an Agilent 34970A measurement station with a 5 m dedicated cable. Figure 6 shows a picture of the probe set-up.



Figure 6: Probe set up.

### 6.1. Cold spot detection experiment

The first experimental test recreates the conditions of the low-temperature defect that can appear due to the proximity of a cold spot, like a defect on a thermal isolation. For that, the cable sample was partially immersed in a tank full of liquid nitrogen. This insured a temperature of  $-195.7^{\circ}\text{C}$  on the immersed part and a small gradient on the close parts of the tank. A first reference measurement was taken at ambient temperature. Then, after immersing the cable, we waited for the temperature to stabilize and proceed to TDR measurements with both VNA and CEA-sensor. Figure 7 presents the schematic of the experiment and the photography of the test-bed.

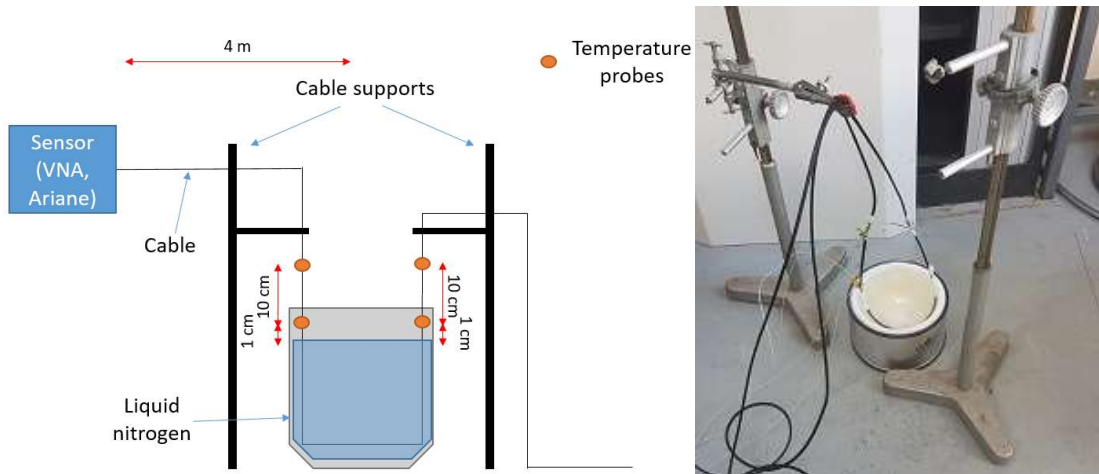


Figure 7: Cold spot detection experiment.

### 6.2. Hot spot detection experiment

The second experimental test recreates the conditions for hot spot appearance on a cable, such as the proximity of a harness to an engine. For that, a part of the cable sample is installed in a controlled oven and different temperature levels over time are set. First, a measurement at ambient temperature is taken as a reference. Then we selected six levels, with the following steps: we set the oven to the first step, waited for the temperature to stabilize, took the reflectometry measurements with both VNA and CEA-Sensor, and then raised the temperature to the next level, and so on. Table 2 presents the temperature levels for the test.

Table 2 : Temperature levels for hot spot experiment.

Level	1	2	3	4	5	6
Temperature	$60^{\circ}\text{C}$	$80^{\circ}\text{C}$	$100^{\circ}\text{C}$	$120^{\circ}\text{C}$	$140^{\circ}\text{C}$	$160^{\circ}\text{C}$

Figure 8 presents the schematic of the experiment and the photography of the Vötsch VT7010 controlled oven used for the experiment.

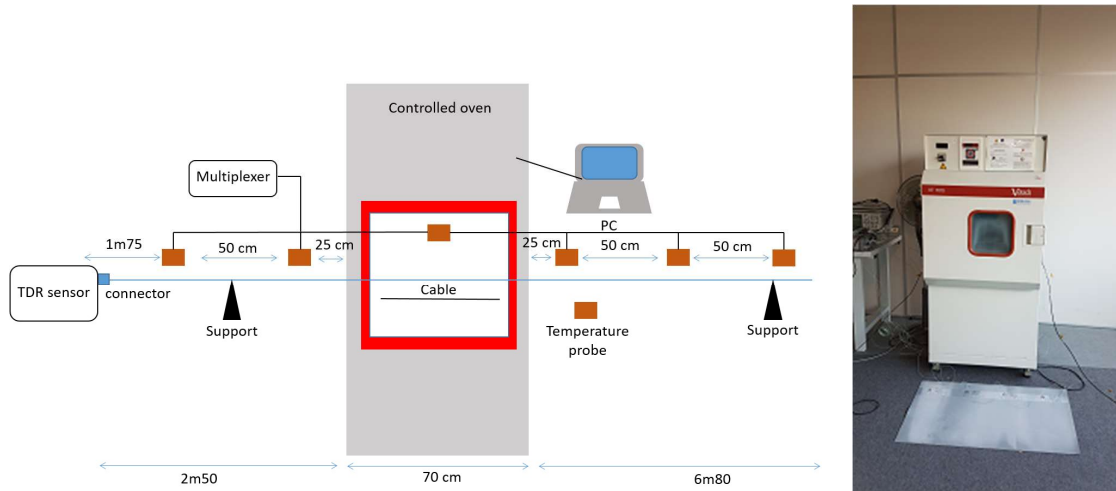


Figure 8: Hot spot detection experiment.

## 6. Experimental results

### 6.1. Cold spot detection

As previously mentioned, three reference measurements (with ambient temperature) and three TDR measurements (with cold spot) are taken using VNA and CEA-sensor. Figure 9 shows the reflectograms. We observe multiple reflections that makes the analysis of the reflectogram a bit difficult. However, we can easily differentiate the signature corresponding to the area immersed in the liquid nitrogen around 150 ns. To facilitate the interpretation, we exploit the differential reflectogram corresponding to the difference between the reference and the measured reflectogram. The results showed on Figure 10 shows how parasitic reflections are removed.

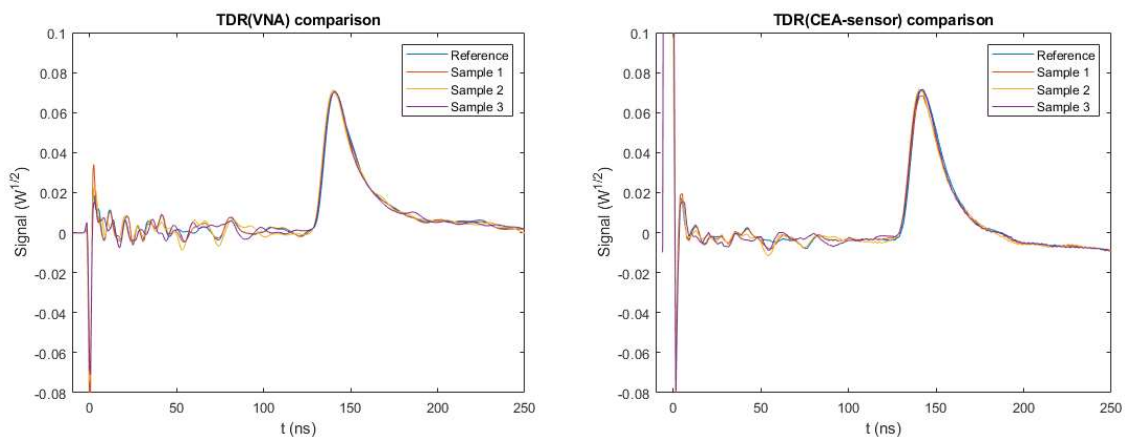


Figure 9: Cold spot TDR results.

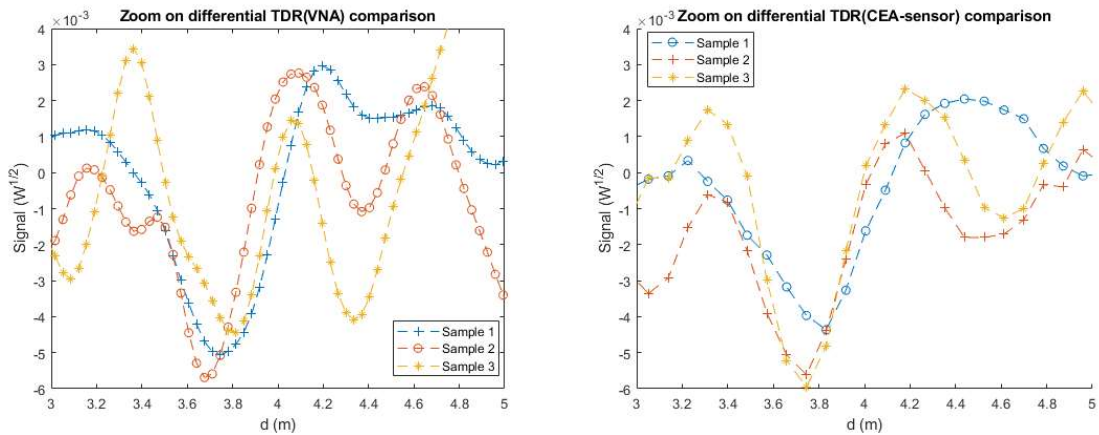


Figure 10: Differential reflectograms for cold spot detection.

The results are still difficult to read, however we can differentiate the signature of the cold spot (around 3.8 m). There is the presence of an alternation of one negative and one positive peak. This is expected because the lower temperature decreases locally the characteristic impedance, which creates a negative reflection coefficient and then a positive one. We think that the variability observed between the samples is mainly due to the variation of the physical installation of the cable during the experiment. Since the reflection levels seems to be low, they are prompt to be mixed to the ones generated by slight curvatures on the cable. This means that even though they are visible and detectable, it will necessitate a specific post-treatment to isolate them completely.

Figure 11 shows the temperature profile given by the temperature probes placed on the cable.

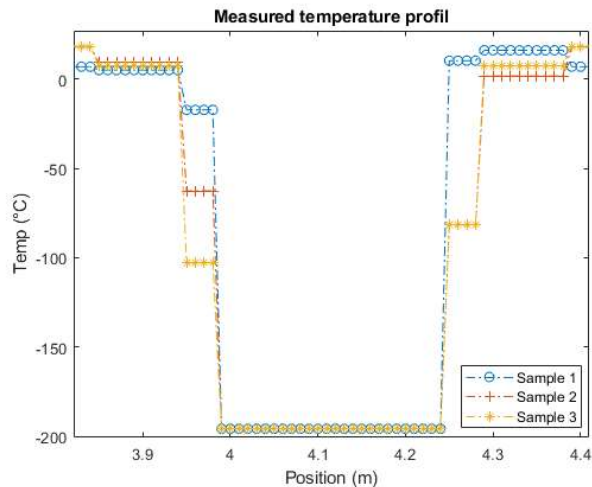


Figure 11: Temperature profile along the cable under test.

## 6.2. Hot spot detection

Figure 12 shows the reflectograms obtained with the VNA and the CEA-Sensor in the case of hot spot detection. The first peak in the reflectogram of the left is due to the reflection due to the impedance mismatch between the sensors and the connector whereas in the case of the VNA measurement, the incipient signal is automatically removed from the trace. The last peak corresponds to the open circuit at the end of the cable. In the middle, we can observe the reflections in the area under stress. In the area of interest, we find one positive and one negative peak, opposite to the previous case, since the higher temperature increases the characteristic impedance.

The temperature probes gave us the temperature measured directly inside the insulation coating and in the area close to the controlled oven. There was a slight gap between the wanted temperature and the real one on the cable. A small gradient of temperature is present over a couple of meters directly outside the oven, as can be seen on Figure 13.

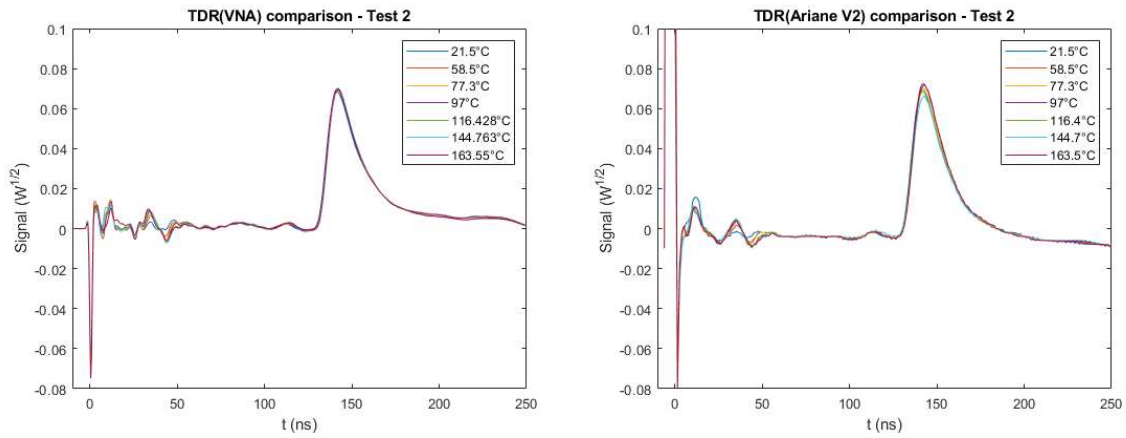


Figure 12 : Hot spot TDR results

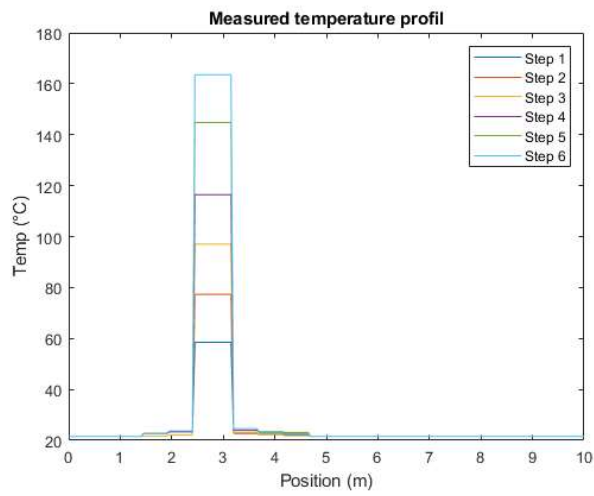


Figure 13: Temperature profile along the cable under test.

Figure 14 shows the differential reflectograms for different temperatures. We can observe that the results are easier to interpret than in the case of cold spot. This is due to the fact that the test-bed is more stable and that the cable does not move between each measurement in the case of this experiment.

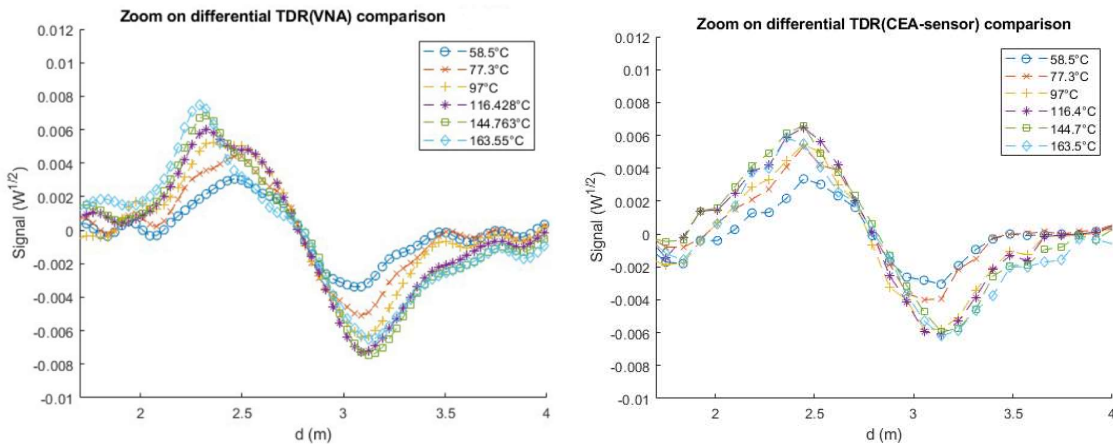


Figure 14: Differential reflectograms for hot spot detection.

## 7. Comparison between simulation and experimental results

Using the new approach for ABCD-modelling, it is possible to recreate the measured temperature profile for both sets of experiments. Thanks to an extraction of the cable propagation parameters, and knowing the law of evolution of these parameters with temperature, we could design the proper mesh and simulate the defect corresponding to each case. Figure 15 (a) and (b) presents the simulations results for the cold spot and hot spot simulations, respectively.

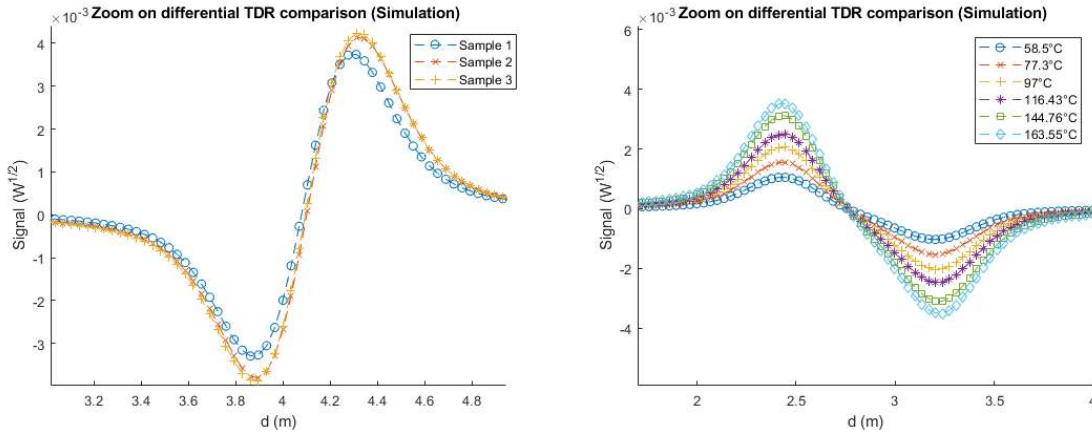


Figure 15: (a) Cold Simulations, (b) hot spot simulations.

We can see a great convergence between the simulations and the experimental results, despite some discrepancies due to environmental perturbations like for instance the curvature of the cable. We can observe that the progressive effect of the temperature for the hot spot is reproduced and the relative positions of the peaks for both cases are respected. However, it seems that the simulation model gives lower reflection coefficients than the measurement. This was expected for cold spot detection due to the presence of other contingent effects. For hot spot simulation, it is probable that we underestimated the variability of the cable components in our model. The cable is more sensitive to the high temperature than we expected. More details on the characteristics of the insulation material would be useful to delve into this discrepancy.

This would be problematic if we wanted to extract from simulation the exact values for defects on a harness, but the model does not aim to be used in that way. It helps us anticipate the capacity of an embedded system to detect the presence of unwanted reflections on the harness. In that case, it represents a worst case in regards to the magnitude of the reflections and remains pertinent to be implemented in other scenarios. The experimental measure remains the reference.

## 8. Conclusion

In this work, we investigated thermal effect modelling on the cable based on an improved ABCD mesh description. We showed that we can get TDR responses without multiple reflections and with reduced noise left by simply choosing the right mesh fineness.

Experimental measurements have been conducted taking into account both cold and hot spot detection. We used a reference device from the market and deployed a CEA-made TDR sensor, designed for embedded diagnosis. Comparing experimental results to simulations, we have been able to validate the proposed approach. We confirmed the pertinence of the new model and demonstrated the capacity of TDR to detect both cold and hot spots.

This work is an important step for future harness's diagnosis systems. With the validated new modelling method, it is now possible to integrate a precise description of temperature defect in simulation tools and anticipate the dimensioning of future diagnosis electronic architectures, such as the sensibility of the sensors, the sampling frequency or the need for post-processing according to the type of constraints during a mission. We are more confident in our previous conclusions in [1]. A simulation work, integrating the new models and other constraints, close to the conditions of missions is in progress and we have good hope now to detect, localize temperature defects and separate them from other sources.

To go further, it would be interesting to reproduce the same experiments to give more statistical meaning to our results, especially for the cold spot experiment, in which we would normalize the position of the cable and remove all curvature effects on the measures. In the same way, with better information on the behaviour of the dielectric component of the cable, we could have a better match between experiment and simulation.

## References

[1] Grégis N. Cartron M. and Monchaux D. 2019. A New Design of an Embedded System for Online Harness Monitoring in Reusable Launch Vehicles Using Reflectometry. 8th European Conference for Aeronautics and Space Sciences (EUCASS).

[2] Furse, C., Chung, Y. C., Dangol, R., Nielsen, M., Mabey, G., & Woodward, R. (2003). Frequency-domain reflectometry for on-board testing of aging aircraft wiring. *IEEE Transactions on Electromagnetic Compatibility*, 45(2), 306-315.

[3] Ben Hassen, W., Auzanneau, F., Peres, F., & Tchangani, A. (2012). A distributed diagnosis strategy using bayesian network for complex wiring networks. *IFAC Proceedings Volumes*, 45(31), 42-47.